Conformational Study of the Alanine Dipeptide at the MP2 and DFT Levels

Rubicelia Vargas,[†] Jorge Garza,[†] Benjamin P. Hay,[‡] and David A. Dixon*[,‡]

Departamento de Química, División de Ciencias Básicas e Ingeniería, Universidad Autonóma Metropolitana-Iztapalapa, A.P. 55-534, México Distrito Federal 09340, México, and William R. Wiley, Environmental Molecular Sciences Laboratory, Pacific Northwest National Laboratory, P.O. Box 999, Richland, Washington 99352

Received: October 25, 2001; In Final Form: December 21, 2001

Conformations of an important model system, the alanine dipeptide, have been calculated by using high-level, ab initio electronic structure theory. A Ramachandran plot, with the angle ϕ in the range −180° to 90° and the angle ψ in the range −60° to 180°, was generated by using density functional theory with the generalized-gradient BLYP functional and a polarized triple-ζ basis set (TZVP+). Six conformers, $C7_{eq}$, C_5, $C7_{ax}$, β_2, α_L, and α', have been identified in this region of the Ramachandran plot. A second derivative (frequency) analysis showed that all conformers are stable at this level of theory. These structures were used as starting points for geometry optimizations at the MP2/aug-cc-pVDZ level. Single-point energies were calculated at the MP2/aug-cc-pVTZ and MP2/aug-cc-pVQZ levels at the final MP2/aug-cc-pVDZ structures and together with the MP2/aug-cc-pVDZ results were used in extrapolations to the complete basis set limit. The N−H···O, N−H···N, and C−H···O hydrogen bond interactions that are key to the energetics are discussed. In general, the results obtained at the BLYP/TZVP+, MP2/aug-cc-pVDZ, MP2/aug-cc-pVTZ//aug-cc-pVDZ, and MP2/aug-cc-pVQZ//aug-cc-pVDZ levels are in reasonable agreement with each other, except for the β_2 conformation for which there are significant differences in the structures. Although the same stability order is obtained at all levels of theory that were used, there are significant differences in the magnitude of the relative conformational energies.

Introduction

Models based on empirical potential functions are widely used to simulate the structural, dynamical, and equilibrium thermodynamic properties of proteins.[1] There are currently several computer programs, for example, AMBER,[2] GROMOS,[3] DISCOVER,[4] CHARMM,[5] ECEPP,[6] and NWChem,[7] that have been developed for such classical simulations of biomolecules. The structures and conformational energies obtained from electronic structure calculations on small peptides provide valuable data with which to parametrize and validate the classical force fields that are used in such codes. The alanine dipeptide, 2-(acetylamino)-*N*-methyl-propanamide, is one of the key molecules that have been used for this purpose.

Several studies have been reported in which electronic structure calculations have been used for the conformational analysis of the alanine dipeptide (**1**)[8−13] and the simpler analogue, 2-(formylamino)propanamide (**2**),[14] in which the terminal methyl groups have been replaced with hydrogens. If it is assumed that each of the two amide bonds are constrained to the more stable trans orientation (in other words, each amide hydrogen atom is trans with respect to the carbonyl oxygen atom),[15] then the conformers of the dipeptides **1** and **2** are fully characterized by the Ramachandran angles ϕ and ψ defined in Figure 1.[16] To date, electronic structure calculations have identified a total of nine distinct conformers for **1** (see Table 1). Six of these conformers, $C7_{eq}$, C5, $C7_{ax}$, β_2, α_L, and α', are present at all levels of theory. An α_R conformer for **1** has been reported at the HF/4-21G and HF/6-31G** levels of theory.[8,10]

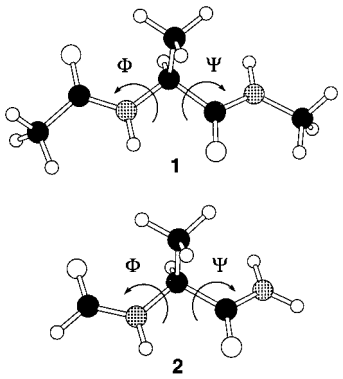

Figure 1. Structure of the alanine dipeptide (**1**) and 2-(formylamino)-propanamide (**2**) with the Ramachandran angles ϕ and ψ indicated. The dihedral angle ϕ is defined as C(O)−N−C_α−C(O) and ψ is defined as N−C_α−C(O)−N for both **1** and **2**.

In contrast, subsequent calculations failed to locate the α_R conformer as a minimum on the HF/6-31G*, B3LYP/6-31G*, or MP2/6-31G* potential energy surfaces.[11] HF/3-21G calculations yielded an α_D conformer for **2**,[14] and HF/6-31G* calculations yielded an α_D conformer for **1**.[11] However, the α_D conformer of **1** could not be found as a minimum on the B3LYP/6-31G* or MP2/6-31G* potential surfaces.[11] Finally, a β conformer for **1** has been reported at the HF/6-31G** level of theory.[10] Subsequent studies have neither confirmed nor denied the presence of a stable β conformer at other levels of theory.

The relative energies that have been reported for the conformers of **1** and **2** are presented in Table 1. For the six conformers of **1** that are present at all levels of theory, it can be seen that the methods that include electron correlation, second-

[†] Universidad Autonóma Metropolitana-Iztapalapa.
[‡] Pacific Northwest National Laboratory.

10.1021/jp013952f CCC: $22.00
Published on Web 03/12/2002

TABLE 1: Relative Energies (kcal/mol) for Conformers of 1 and 2 Reported at Different Levels of Theory[a]

			1										2		
conformer	Φ range (deg)	Ψ range (deg)	HF/4-21G//HF/4-21G (ref. 8)	HF/DZP//HF/DZP (ref. 9)	HF/6-31G*//HF/6-31G* (ref. 11)	HF/6-31G**//HF/6-31G** (ref. 10)	MP2/TZVP//HF/6-31G** (ref. 10)	MP2/6-31G*//MP2/6-31G* (ref. 11)	MP2/cc-pVTZ//MP2/6-31G* (ref. 13)	MP4+BSSE/cc-pVTZ(-f)//MP2/6-31G* (ref. 13)	B3LYP/6-31G*//B3LYP/6-31G* (ref. 11)	BPE//BPE (ref. 12)	HF/3-21G//HF/3-21G (ref. 14)	HF/6-31+G*//HF/6-31+G* (ref. 14)	MP2/6-31+G*//HF/6-31+G* (ref. 14)
$C7_{eq}$	-81 to -86	66 to 79	0.0	0.00	0.00	0.00	0.00	0.00	0.00	0.00	0.00	0.00	0.00	0.00	0.00
C5	-156 to -168	159 to 171	1.4	0.50	0.41	0.40	1.47	1.76	1.61	0.89	1.43	1.97	1.26	0.19	1.13
$C7_{ax}$	72 to 76	-54 to -62	2.6	2.99	2.82	2.82	2.05	2.58	2.41	2.55	2.61	2.36	2.53	2.56	2.19
β_2	-110 to -136	12 to 38	3.9		2.58	2.58	3.25	3.37	3.27	2.56	3.18	3.88	3.83	2.24	2.67
α_R	-61 to -92	-5 to -41	4.9		NOT	4.35	3.91	NOT			NOT				
α_L	63 to 70	19 to 41	6.7	4.42	4.72	4.76	4.42	4.60	4.38	4.21	5.82	5.74	5.95	4.73	4.46
β	-58	134				4.90	4.08								
α'	-161 to -179	-41 to -55	7.9		5.74	5.81		6.34	5.49	5.17	6.85		7.31	5.52	5.83
α_D	57 to 68	-133 to -177			4.82			NOT			NOT		8.16	NOT	

[a] NOT indicates that the conformer was investigated and found not to be a minimum at this level of theory.

and fourth-order Møller−Plesset (MP2 and MP4),[17] and density functional theory (DFT)[18] all yield the same relative order of stability, $C7_{eq} < C5 < C7_{ax} < \beta_2 < \alpha_L < \alpha'$, for all of the basis sets used. In addition, the stability order at the MP2 level is independent of whether the geometry was optimized at the Hartree−Fock (HF) level or the MP2 level. The simpler analogue, **2**, yields the same six conformations with the same stability order, demonstrating that removal of the terminal methyl groups does not greatly affect the potential surface for rotation about ϕ and ψ. Although the relative order of the conformers remains constant at the higher levels of theory, there are significant differences in the relative energies. For example, comparison of the results obtained at the best level of theory, MP4+BSSE/cc-pVTZ(-f)//MP2/6-31G*, with those obtained at MP2/6-31G*//MP2/6-31G* reveals relative energy differences in excess of 1 kcal/mol.

Advances in computational capability, including massively parallel (MPP) hardware, software that runs efficiently on such MPP architectures,[7] new algorithms, and new basis sets that can be extrapolated to the complete basis set (CBS) limit,[19] now make it possible to obtain highly accurate energetic information about molecular conformations and hydrogen-bond interactions for a given level of treatment of the correlation energy. There is a clear gap between the results that have been reported up to now for **1** and the results that can be obtained with current technology and basis sets. In this paper, we report the structures and energies of the stable conformations of **1** obtained by using the MP2 method with a large basis set. In addition, we use these results to benchmark the performance of DFT with the GGA exchange-correlation functional BLYP[20] for **1**. We have used this exchange-correlation functional because it is a popular functional for quantum chemistry with formal scaling as N^3 when charge fitting is used.

Computational Methods

A Ramachandran plot for **1** was generated with DFT calculations performed by using the DGauss program.[21] Constrained optimizations were performed with the BLYP exchange-correlation functional[20] by using a polarized triple-ζ basis set and the A2 fitting basis set (TZVP+).[22] The Ramachandran plot was generated from an equally spaced grid of 304 points. By using a step size of 15° for each angle, ϕ was varied from −180° to 90° and ψ was varied from −60° to 180°. These angle ranges were chosen to yield a potential surface that would contain all previously reported conformers with the exception of the putative α_D form. Although ϕ and ψ were constrained during these optimizations, all other degrees of freedom were optimized at each point yielding a fully relaxed potential surface. Minima observed at the following positions were then subjected to full optimizations (ϕ, ψ): (−75°, 75°); (−150°, 150°); (75°, −60°); (−120°, 30°); (75°, 30°); (−175°, −30°).

To generate initial geometries for the α_D form, constrained BLYP/TZVP+ geometry optimizations were performed on **1** ($\phi = 57.3°$, $\psi = -133.5°$), the structure previously located at the HF/6-31G* level,[11] and ($\phi = 67.5°$, $\psi = -177.3°$), the structure previously located with HF/3-21G optimization.[14] Although not observed on the Ramachandran plot, constrained BLYP/TZVP+ geometry optimizations were also performed to generate initial geometries for the α_R form ($\phi = -60.7°$, $\psi = -40.7°$) and the β form ($\phi = -57.6°$, $\psi = 134.4°$) reported at the HF/6-31G** level.[10]

After removal of the dihedral angle constraints, full geometry optimizations at the BLYP/TZVP+ level were performed on the initial geometries of minima selected either from the Ramachandran grid or created for the α_D, α_R, and β forms. All optimized structures were characterized by computing second derivatives. The absence of imaginary (negative) frequencies confirmed that all final, optimized structures are minima.

MP2(Full) calculations were carried out with the aug-cc-pVDZ, aug-cc-pVTZ, and aug-cc-pVQZ basis sets[19] by using the NWChem program.[7] The BLYP/TZVP+ geometries were used as starting geometries for optimizations at the MP2/aug-cc-pVDZ level. Single-point calculations were carried out at the MP2/aug-cc-pVTZ and MP2/aug-cc-pVQZ levels at the MP2/aug-cc-pVDZ geometries. The CBS limit was obtained by extrapolating the total energies, MP2/aug-cc-pVXZ for X = D, T, and Q, of each conformer by using a mixed Gaussian exponential extrapolation.[23]

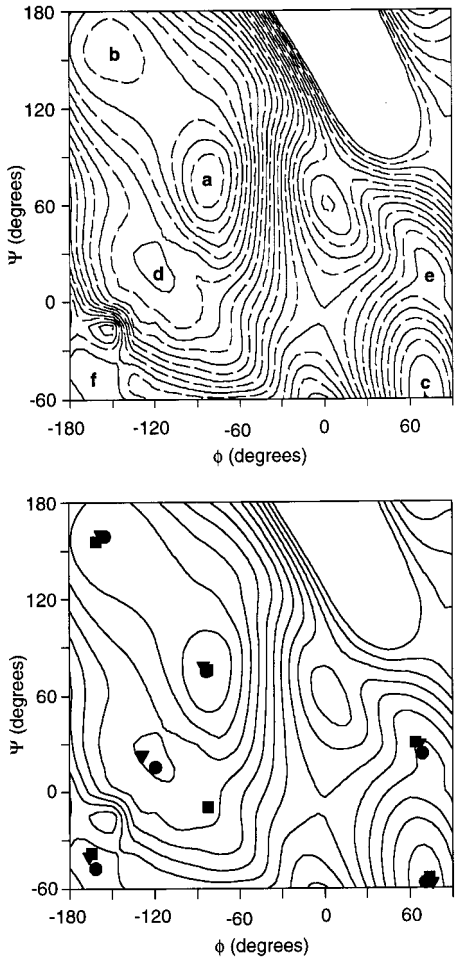

Figure 2. The BLYP/TZVP+ Ramachandran plot for **1** (top) obtained from a grid of points with 15° spacing. Minima are labeled as follows: a ($C7_{eq}$), b (C5), c ($C7_{ax}$), d (β_2), e (α_L), and f (α'). The solid contours are drawn every 1.0 kcal/mol and the dashed lines between them are drawn every 0.5 kcal/mol. The energy scale goes from zero (for the most stable conformation, $C7_{eq}$) to 12.0 kcal/mol. The bottom panel shows the location of the minima on the BLYP/TZVP+ Ramachandran plot after optimization at the BLYP/TZVP+ (●), MP2/aug-cc-pVDZ (■), and HF/6-31G** (▼)[9] levels of theory. The solid contours are drawn every 1.0 kcal/mol.

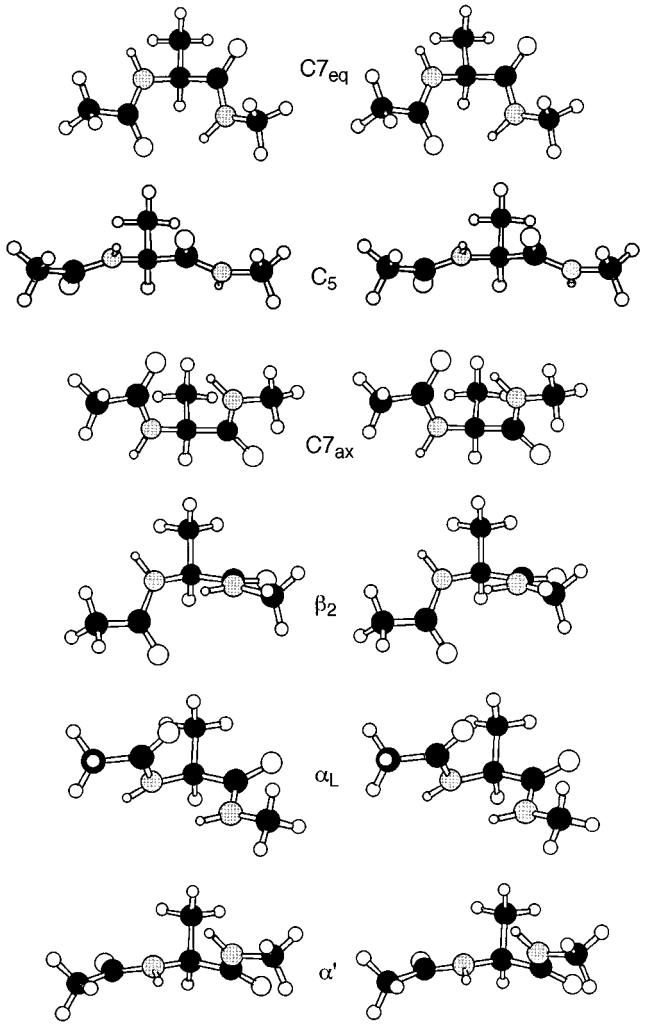

Figure 3. Stereoviews of the six minima of **1** after optimization at the MP2/aug-cc-pVDZ level.

TABLE 2: Ramachandran Dihedral Angles ϕ and ψ (deg) for 1

conformer	dihedral	HF[a]	MP2[b]	B3LYP[c]	BLYP[d]	MP2[e]
$C7_{eq}$	ϕ	−85.8	−83.1	−81.9	−83.8	−82.6
	ψ	78.5	77.8	72.7	75.1	75.8
C5	ϕ	−157.9	−158.4	−157.3	−155.0	−161.1
	ψ	160.3	161.3	165.3	158.8	155.5
$C7_{ax}$	ϕ	75.8	74.4	73.8	70.8	73.7
	ψ	−56.5	−64.2	−60.0	−56.6	−53.7
β_2	ϕ	−128.6	−137.9	−135.9	−119.6	−82.3
	ψ	23.2	22.9	23.4	15.3	−9.5
α_L	ϕ	66.9	63.5	68.2	68.7	63.8
	ψ	29.7	34.8	24.7	23.3	30.2
α'	ϕ	−166.4	−166.1	−169.4	−161.8	−164.7
	ψ	−40.1	−37.2	−37.8	−47.6	−38.3

[a] HF/6-31G** (ref 10). [b] MP2/6-31G* (ref 13). [c] B3LYP/6-31G* (ref 11). [d] BLYP/TZVP+ (this work). [e] MP2/aug-cc-pVDZ (this work).

Results and Discussion

The Ramachandran plot for **1** obtained at the BLYP/TZVP+ level is depicted in Figure 2 (top). The ϕ and ψ angles for the six minima observed in this plot are shown in Figure 3, and their ϕ and ψ angles are summarized in Table 2. Three low-energy minima are clearly observed in the diagram. Two of them are between ϕ from −180° to −60° and ψ from 45° to 180°, corresponding to the $C7_{eq}$ and C5 conformations. The third is localized on the left bottom of the diagram and corresponds to the $C7_{ax}$. Three higher-energy minima are also observable. A β_2 conformation lies in a very flat, large region in the range of 3−4 kcal/mol. Finally, higher-energy α_L and α' conformers are observed in the expected regions of the plot.

The α_R and β conformers previously reported at the HF level of theory are not present in the Ramachandran plot. Attempts to locate them at the BLYP/TZVP+ level, starting from $\phi = -60.7°$ and $\psi = 40.7°$ for α_R and $\phi = -57.6°$ and $\psi = 134.4°$ for β, failed. In the optimization process, the former starting geometry yielded the β_2 conformation and the latter starting geometry yielded the $C7_{eq}$ conformation. Although a third previously reported conformer, α_D, is outside the range of the mapped region, attempts to locate this conformation at the BLYP/TZVP+ level of theory failed. When started from either $\phi = 57.3°$ and $\psi = -133.5°$ or $\phi = -67.5°$ and $\psi = -177.3°$, the $C7_{ax}$ conformation is obtained.

In summary, the BLYP/TZVP+ calculations were able to locate only six stable conformers: $C7_{eq}$, C5, $C7_{ax}$, β_2, α_L, and α'. Second derivative analyses on these conformations establish all structures to be minima at this level of theory. Taking the

TABLE 3: Relative Energies for Conformers of 1 (kcal/mol)

Conformer	LMP2/cc-pVTZ(-f)// MP2/6-31G** (ref. 13).	MP2/cc-pVTZ(-f)// MP2/6-31G* (ref. 13).	B3LYP/6-31G* (ref. 11).	BLYP/TZVP+ (this work)	MP2/aug-cc-pVDZ// BLYP/TZVP+ (this work)	MP2/aug-cc-pVDZ (this work)	MP2/aug-cc-pVTZ// MP2/aug-cc-pVDZ (this work)	MP2/aug-cc-pVQZ// MP2/aug-cc-pVDZ (this work)	MP2/CBS limit// MP2/aug-cc-pVDZ (this work)	MP4+BSSE/cc-pVTZ(-f)// MP2/6-31G* (ref. 13)	MP4/cc-pVTZ(-f)// MP2/6-31G* (ref. 13)
$C7_{eq}$	0.00	0.00	0.00	0.00	0.00	0.00	0.00	0.00	0.00	0.00	0.00
C5	1.11	1.61	1.43	1.16	1.77	1.91	1.87	1.59	1.39	0.89	1.39
$C7_{ax}$	2.48	2.41	2.61	2.46	2.36	2.28	1.96	2.37	2.66	2.55	2.48
β_2	2.78	3.27	3.18	2.78	3.36	3.11	3.00	3.21	3.35	2.56	3.05
α_L	4.36	4.38	5.82	5.81	5.02	4.50	4.59	4.95	5.19	4.21	4.23
α'	5.49	5.94	6.34	6.67	6.88	6.51	6.59	6.72	6.80	5.17	5.62

BLYP/TZVP+ geometries as starting points, we further optimized the six conformers at the MP2/aug-cc-pVDZ. The location of the minima from both levels of theory tested in this work and from prior HF calculations are shown on the Ramachandran plot in Figure 2 (bottom). With the exception of the β_2 conformation, all three levels of theory yield very similar structures. When compared with the BLYP result, the β_2 conformation obtained at the MP2 level differs by 37° in ϕ and 25° in ψ, and we note that this is in a very flat region of the potential energy surface.

Relative energies of the six conformers at seven different levels of theory are listed in Table 3, together with the extrapolation to the CBS limit. In all cases, the same order of stability is obtained: $C7_{eq} < C5 < C7_{ax} < \beta_2 < \alpha_L < \alpha'$. The two gradient-corrected DFT methods give energies that differ at most by 0.40 kcal/mol, which is found for the β_2 conformer. Thus, the inclusion of Hartree−Fock exchange in the B3LYP/6-31G* calculations does not appear to give a large difference in the relative energies with respect to the BLYP/TZVP+ level. By comparing the relative energies obtained at the BLYP/TZVP+ and MP2/aug-cc-pVXZ levels, we find that the biggest difference, 1.31 kcal/mol, occurs with the α_L conformation at the MP2/aug-cc-pVDZ level. The result is a closer relative energy between the α_L and β_2 conformations at the MP2/aug-cc-pVDZ level. At the BLYP/TZVP+ level, the β_2 form is 3.03 kcal more stable than the α_L form, whereas at the MP2/aug-cc-pVDZ level, the β_2 form is only 1.39 kcal more stable than the α_L form. This difference is due in part to the optimization and in part to the method itself. Overall, the differences in the MP2/aug-cc-pVDZ//BLYP/TZVP+ and the MP2/aug-cc-pVDZ results are small with the largest difference of 0.5 kcal/mol for the α_L conformer. Although the difference in energy between the β_2 and α_L conformers increases at the MP2 level with larger basis sets, the increase is not large enough to approach the difference obtained at the BLYP/TZVP+ level as even at the MP2/CBS limit, the β_2 conformer is more stable than the α_L form by only 1.84 kcal/mol. Another difference in relative energies is found for the C5 and $C7_{ax}$ conformers for which the BLYP/TZVP+ difference is 1.30 kcal/mol and the MP2/aug-cc-pVDZ difference is 0.37 kcal/mol. This difference is sensitive to the basis set at the MP2 level: 0.09 kcal/mol with the aug-cc-pVTZ basis set, 0.78 with the aug-cc-pVQZ basis set and 1.27 kcal/mol at the CBS limit.

The best available results from our calculations are the MP2/CBS results. These results do not have any basis set superposition error (BSSE) because they are at the CBS limit. BSSE might be expected to play a role in the energetics for smaller basis sets as the structures range from extended to more compact. The MP2/CBS energy results for the energies of the C5, $C7_{ax}$, and β_2 conformers relative to the $C7_{eq}$ conformer are within 0.2 kcal/mol of the MP2/cc-pVTZ(-f)//HF/6-31G** and B3LYP/6-31G* results and within 0.5 kcal/mol of the BLYP/TZVP+ and MP2/cc-pVDZ results. The largest differences are found for the β_2 conformer at the BLYP/TZVP+ level and the C5 conformer at the MP2/cc-pVDZ level. The relative energies of the α_L and α' conformers with the different methods show larger variations of up to 1 kcal/mol relative to the MP2/CBS limit results. The MP4+BSSE/cc-pVTZ(-f)//MP2/6-31G* results show quite large deviations from the MP2/CBS limit results. The differences are up to 1.6 kcal/mol, and all of the MP4 energy differences are smaller than the MP2/CBS limit results. The only value in good agreement is the energy difference between the $C7_{eq}$ and $C7_{ax}$ conformers. However, the MP4/cc-pVTZ(-f) results for the relative energies of the first four conformers are in good agreement with our MP2/CBS results within 0.3 kcal/mol. The highest energy conformers show larger deviations at the MP4/cc-pVTZ(-f) level. The MP4 values are a composite based on an MP4(SDQ) calculation with a modified 6-31G** basis set added to MP2/cc-pVTZ(-f) results. The BSSE contribution is due to taking the difference between "local MP2 (LMP2)" and MP2 calculations with this basis set assuming that the LMP2 calculations handle BSSE corrections better. On the basis of our CBS results, which account for the BSSE effect, the MP2 results are closer to the correct values as compared to the LMP2 results, which apparently overestimate the BSSE correction. This manifests itself in the MP4 results as well. Thus, we feel that our MP2/CBS results provide the best estimate of the relative conformational energetics of the alanine dipeptide.

Internal hydrogen bonds play a role in stabilizing the different conformations of **1**. Three types of internal hydrogen bonds, N−H···O, N−H···N, and C−H···O, are present. Calculated hydrogen-bond energies for *N*-methylacetamide dimers and *N*-methylacetamide/methane dimers establish the following stability order for these interactions: N−H···O (−8.6 kcal/mol) > N−H···N (−1.6 kcal/mol) > C−H···O (−0.5 kcal/mol).[24,25] However, it has been shown that when the hydrogen donor is made more acidic by the presence of electron-withdrawing groups, C−H···O hydrogen bonds can increase in strength from −1.0 to −3.0 kcal/mol,[26] which are within the same range or stronger than the N−H···N interaction. Although the weaker

TABLE 4: Structural Parameters for Hydrogen Bonds in MP2/aug-cc-pVDZ Geometries[a]

	$C7_{eq}$	C5	$C7_{ax}$	β_2	α_L	α'
			N−H···O Hydrogen Bond			
r(H···O)	2.02	2.23	1.88	2.95	2.85	NP
r(N···O)	2.91	2.68	2.82	3.40	3.13	NP
∠N−H···O	144.8	105.0	151.7	108.4	96.7	NP
∠C═O···H	104.8	84.7	103.2	63.4	67.5	NP
			N−H···N Hydrogen Bond			
r(H···N)	NP	NP	2.70	2.27	2.30	2.48
r(N···N)	NP	NP	2.97	2.75	2.77	2.76
∠N−H···N	NP	NP	95.1	107.2	106.9	95.0
∠H···N−C	NP	NP	65.9	89.0	87.7	76.0
			C−H···O Hydrogen Bond[b]			
r(H···O)	2.65	2.37	2.48	2.65	2.64	2.48
	2.68	2.53		2.60	2.55	2.64
	2.48			2.53	2.54	2.69
r(C···O)	2.81	2.85	3.08	2.98	2.77	3.10
	2.79	2.77		2.79	2.81	2.77
	2.81			2.79	3.13	2.78
∠C−H···O	87.0	104.1	113.5	96.3	85.1	113.9
	84.0	90.7		87.7	92.1	85.1
	95.5			91.7	112.9	83.2
	72.8	82.1	97.7	76.9	79.2	97.1
∠C═O···H	77.5	80.1		79.1	84.4	79.2
	104.8			76.9	90.8	76.5

[a] Distances in Å, angles in deg. NP = Not present. [b] Data presented only for C−H···O contacts in which the H···O distance is ≤2.7 Å.

N−H···N and C−H···O interactions are expected to contribute to the stability of a given conformation, the stronger N−H···O hydrogen bond should play the dominant role in determining the relative stabilities of the conformations.

Examination of the hydrogen bonding in the conformers of **1** supports this hypothesis. Geometric parameters for the hydrogen-bond interactions in the MP2/aug-cc-pVDZ optimized geometries are given in Table 4. It can be seen that the three most stable conformations, $C7_{eq}$, C5, and $C7_{ax}$, all contain short N−H···O hydrogen bonds. However, the N−H···O hydrogen bonds do not completely govern the relative energetics as other steric interactions are present, which contribute to the energy differences. Those structures with longer N−H···O contacts, the β_2 and α_L conformers, are less stable, and the least stable conformer, α', lacks a N−H···O interaction altogether. The geometric parameters of the N−H···O hydrogen bond are not favorable for the β_2 and α_L conformers, but in these conformers, the N−H···N hydrogen bond contacts are nearer to the optimal hydrogen-bond geometrical parameters, showing that this interaction plays a role in stabilizing both conformers. For all conformers, C−H···O hydrogen bond interactions are present, and although this is a weak interaction, it can be important for the stabilization of some systems. As shown in Table 4, favorable hydrogen-bond parameters for this weak bond are found in the all conformers and, these are the interactions that are important in the stabilization of the α' conformation.

As noted above, the geometric parameters for the β_2 conformation are the only ones that show a dependence on the computational method. The energy for the β_2 conformation at the MP2/aug-ccpVDZ level is only 0.33 kcal/mol above that obtained at BLYP/TZVP+ level even though we found that the Ramachandran angles between them were very different. As noted above, this is due to the flat region observed in the Ramachandran plot where the β_2 conformer is found. For example, for the β_2 conformer, the relative energy at the MP2/aug-ccpVDZ//MP2/aug-ccpVDZ level is lower by only 0.25 kcal/mol as compared to that at the MP2/aug-ccpVDZ//BLYP/TZVP+ level even though the dihedral angles for the two optimized geometries are quite different. For the β_2 conformation, the HF/6-31G**, MP2/6-31G*, and BLYP/TZVP+ methods predict a positive value for ψ between 15° and 25° and an average value of $-129° \pm 10°$ for the angle ϕ. At the MP2/aug-cc-pVDZ level, the angle ψ is approximately −10° and ϕ is equal to −82° degrees. The main factors leading to the differences in the structural predictions between the MP2/aug-cc-pVDZ level and the HF/6-31G**, MP2/6-31G*, and BLYP/TZVP+ levels are the size of the basis set and the treatment of the correlation energy. To further check the effect of the basis set on the β_2 conformation, we also performed calculations at the HF and BLYP levels with the aug-cc-pVDZ basis set. The BLYP/aug-cc-pVDZ results ($\phi = -117.0°$ and $\psi = 14.0°$) are essentially the same as the BLYP/TZVP+ ones. The HF/aug-cc-pVDZ results show a larger basis set dependence with the larger basis set results ($\phi = -101.9°$ and $\psi = 4.2°$) moving halfway toward the MP2/aug-cc-pVDZ results showing a significant basis set effect at this level. The remainder of the difference is due to correlation effects. In Table 5, we compare the hydrogen-bond parameters at the MP2 and BLYP levels by using the aug-cc-pVDZ basis set. As shown in this table, the N−H···N interaction has similar geometry parameters at both levels of theory. The main difference between the BLYP and MP2 β_2 geometries is the N−H···O interaction, which is strongly dependent on the theoretical level. The MP2 geometry has a N−H···O hydrogen-bond distance of 2.95 Å, whereas the BLYP calculation yields a very long hydrogen-bond distance of 3.51 Å suggesting that there is little, if any, stabilization at the BLYP level. The reduction in the H···O distance affects mostly the dihedral angles ϕ and ψ. Thus, the method used to describe the N−H···O interaction energy must be good enough to get this interaction correct to compete with the geometrical changes in the parameters ϕ and ψ, which induce strain.

TABLE 5: Hydrogen-Bond Distances (Å) for the β_2 Conformation, Comparison between MP2 and BLYP Calculations with the aug-cc-pVDZ Basis Set

parameter	MP2	BLYP
	N−H···O	
H···O	2.95	3.51
N···O	3.40	4.08
	N−H···N	
H···N	2.27	2.30
N···N	2.75	2.78
	C−H···O	
H···O	2.60	2.43
	2.65	2.56
	2.53	2.36
C···O	2.79	2.86
	2.98	2.90
	2.79	2.87

Conclusions

The geometries of the $C7_{eq}$, C5, $C7_{ax}$, β_2, α_L, and α' conformers of the alanine dipeptide were optimized with two levels of theory, BLYP/TZVP+ and MP2/aug-cc-pVDZ. Both methods give similar results except for the β_2 conformer, and they are in agreement with previous reports. For the most stable $C7_{eq}$, C5, and $C7_{ax}$ conformers, the N−H···O hydrogen-bond interaction is responsible for the stabilization; however, this is not true for the remaining stable conformers. In particular, the β_2 conformer is localized in a very flat region and N−H···N and C−H···O hydrogen-bond interactions are present. Although the BLYP/TZVP+ and MP2/aug-cc-pVDZ methods predict a similar relative energy for this conformer with respect

to the most stable conformer, the geometries are quite different. Complete basis set MP2 results were calculated, and the relative energies for the various conformations relative to the $C7_{eq}$ structure in kcal/mol are as follows: C5, 1.39; $C7_{ax}$, 2.66; β_2, 3.35; α_L, 5.19; α', 6.80. These represent the most accurate values available for the relative energies of the conformers and can be used in the development of molecular force fields for molecular dynamics simulations.

Acknowledgment. Financial support for R.V. and J.G. was partially provided by CONACYT, México. This work was sponsored in part by the Office of Biological and Environmental Research in the U. S. Department of Energy. This research was performed in part by using the Molecular Science Computing Facility (MSCF) in the William R. Wiley Environmental Laboratory at the Pacific Northwest National Laboratory. The MSCF is funded by the Office of Biological and Environmental Research in the U. S. Department of Energy. Pacific Northwest National Laboratory is operated by Battelle for the U. S. Department of Energy under contract DE-AC06-76RLO 1830.

Supporting Information Available: Cartesian coordinates and energies (hartree) for the BLYP/TZVP+ and MP2/aug-cc-pVDZ optimized geometries plus MP2 total energies as a function of basis set.

References and Notes

(1) (a) Brooks, C. L., III; Karplus, M.; Pettitt, B. M. *Proteins, A Theoretical Perspective of Dynamics, Structure, and Thermodyamics*; Advances in Chemical Physics, Vol. LXXI; Wiley: New York, 1988. (b) Levitt, M. *Curr. Opin. Struct. Biol.* **1991**, *1*, 224. (c) Dill, K. A. *Curr. Biol.* **1993**, *3*, 9. (d) Karplus, M.; Sali, A. *Curr. Opin. Struct. Biol.* **1995**, *5*, 58. (e) Vasquez, M.; Nemethy, G.; Scheraga, H. A. *Chem. Rev.* **1994**, *94*, 2183. (f) Dill, K. A.; Bromberg, S.; Yue, K.; Fiebig, K. M.; Yee, D. P.; Thomas, P. D.; Chan, H. S. *Protein Sci.* **1995**, *4*, 561. (g) Jernigan, R. L.; Bahar, I. *Curr. Opin. Struct. Biol.* **1996**, *6*, 195. (h) Friesner, R.; Gunn, J. R. *Annu. Rev. Biophys. Biomol. Struct.* **1996**, *25*, 315. (i) Skolnick, J.; Kolinski, A. In *Encyclopedia of Computational Chemistry*; v. Schleyer, P., Clark, T., Gasteiger, J., Kollman, P. A., Schaefer, H. F. III, Schreiner, P. R., Eds.; John Wiley & Sons: Chichester, U.K., 1998.

(2) (a) Weiner, S. J.; Kollman, P. A.; Case, D. A.; Singh, U. C.; Ghio, C.; Alagona, G.; Profeta, S.; Weiner, P. *J. Am. Chem. Soc.* **1984**, *106*, 765. (b) Weiner, S. J.; Kollman, P. A.; Nguyen, D. T.; Case, D. A. *J. Am. Chem. Soc.* **1986**, *7*, 230.

(3) Van Gunsteren, W. F.; Berendsen, H. J. C.; Hermans, J.; Hol, W. G. J.; Postma, J. P. M. *Proc. Natl. Acad. Sci. U.S.A.* **1983**, *80*, 4313.

(4) (a) Stern, P. S.; Chorev, M.; Goodman, M.; Hagler, A. T. *Biopolymers* **1983**, *22*, 1885. (b) Dauber-Osguthorpe, P.; Roberts, V. A.; Osguthorpe, D. J.; Wolff, J.; Genest, M.; Hagler, A. T. *Proteins* **1988**, *4*, 31.

(5) (a) Brooks, B. R.; Bruccoleri, R. E.; Olafson, B. D.; States, D. J.; Swaminathan, S.; Karplus, M. *J. Comput. Chem.* **1983**, *4*, 187. (b) Pettitt, B. M.; Karplus, M. *Chem. Phys. Lett.* **1985**, *121*, 194. (c) Mackerell, A. D., Jr.; Wiorkiewicz-Kuczera, J.; Karplus, M. *J. Am. Chem. Soc.* **1995**, *117*, 11946.

(6) Roterman, I. K.; Lambert, M. H.; Gibson, K. D.; Scheraga, H. A. *J. Biomol. Struct. Dyn.* **1989**, *7*, 421.

(7) Bernholdt, D. E.; Apra, E.; Fruchtl. H. A.; Guest, M. F.; Harrison, R. J.; Kendall, R. A.; Kutteh, R. A.; Long, X.; Nicholas, J. B.; Nichols, J. A.; Taylor, H. L.; Wong, A. T.; Fann, G. I.; Littlefield, R. J.; Nieplocha, J. *Int. J. Quantum Chem., Quantum Chem. Symp.* **1995**, *29*, 475. Kendall, R. A.; Aprà, E.; Bernholdt, D. E.; Bylaska, E. J.; Dupuis, M.; Fann, G. I.; Harrison, R. J.; Ju, J.; Nichols, J. A.; Nieplocha, J.; Straatsma, T. P.; Windus, T. L.; Wong, A. T. *Comput. Phys. Commun.* **2000**, *128*, 260. Harrison, R. J.; Nichols, J. A.; Straatsma, T. P.; Dupuis, M.; Bylaska, E. J.; Fann, G. I.; Windus, T. L.; Aprà, E.; Anchell, J.; Bernholdt, D.; Borowski, P.; Clark, T.; Clerc, D.; Dachsel, H.; de Jong, B.; Deegan, M.; Dyall, K.; Elwood, D.; Fruchtl, H.; Glendenning, E.; Gutowski, M.; Hess, A. C.; Jaffe, J.; Johnson, B.; Ju, J.; Kendall, R. A.; Kobayashi, R.; Kutteh, R.; Lin, Z.; Littlefield, R.; Long, X.; Meng, B.; Nieplocha, J.; Niu, S.; Rosing, M.; Sandrone, G.; Stave, M.; Taylor, H.; Thomas, G.; van Lenthe, J.; Wolinski, K.; Wong, A.; Zhang, Z. *NWChem, A Computational Chemistry Package for Parallel Computers*, version 4.0.1; William R. Wiley Environmental Molecular Sciences Laboratory, Pacific Northwest National Laboratory: Richland, WA, 2001.

(8) (a) Scarsdale, J. N.; Van Alsenoy, C.; Klimkowski, V. J.; Schäfer, L.; Momany, F. A. *J. Am. Chem. Soc.* **1983**, *105*, 3438. (b) Schäfer, L.; Van Alsenoy, C.; Klimkowski, V. J.; Scarsdale, J. N. *J. Phys. Chem.* **1982**, *76*, 1439.

(9) Böhm, H.-J.; Brode, S. *J. Am. Chem. Soc.* **1991**, *113*, 7129.

(10) (a) Gould, I. R.; Kollman, P. A. *J. Phys. Chem.* **1992**, *96*, 9255. (b) Gould, I. R.; Cornell, W. D.; Hillier, I. H. *J. Am. Chem. Soc.* **1994**, *116*, 9250. (c) Philipp, D. M.; Friesner, R. A. *J. Comput. Chem.* **1999**, *20*, 1468.

(11) Jalkanen, K. J.; Suhai, S. *Chem. Phys.* **1996**, *208*, 81.

(12) Kaschner, R.; Hohl, D. *J. Phys. Chem. A* **1998**, *102*, 5111.

(13) Beachy, M. D.; Chasman, D.; Murphy, R. B.; Halgren, T. A.; Friesner, R. A. *J. Am. Chem. Soc.* **1997**, *119*, 5908.

(14) Head-Gordon, T.; Head-Gordon, M.; Frisch, M. J.; Brooks, C. L., III; Pople, J. A. *J. Am. Chem. Soc.* **1991**, *113*, 5989.

(15) (a) Jorgensen, W. L.; Gao, J. *J. Am. Chem. Soc.* **1988**, *110*, 4212. (b) Schnur, D. M.; Yuh, Y. H.; Dalton, D. R. *J. Org. Chem.* **1989**, *54*, 3779. (c) Lii, J.-H.; Allinger, N. L. *J. Comput. Chem.* **1991**, *12*, 186. (d) Dixon, D. A.; Dobbs, K. D.; Valentini, J. J. *J. Am. Chem. Soc.* **1994**, *98*, 13435.

(16) Ramakrishnan, C.; Ramachandran, G. N. *Biophys. J.* **1965**, *5*, 909.

(17) (a) Møller, C.; Plesset, M. S. *Phys. Rev.* **1934**, *46*, 618. (b) Pople, J. A.; Binkley, J. S.; Seeger, R. *Int. J. Quantum Chem., Quantum Chem. Symp.* **1976**, *10*, 1.

(18) Parr, R. G.; Yang, W. *Density-Functional Theory of Atoms and Molecules*; Oxford University Press: New York, 1989.

(19) (a) Dunning, T. H., Jr. *J. Chem. Phys.* **1989**, *90*, 1007. (b) Kendall, R. A.; Dunning, T. H., Jr.; Harrison, R. J. *J. Chem. Phys.* **1992**, *96*, 6769.

(20) (a) Becke, A. D. *Phys. Rev. A* **1988**, *38*, 3098. (b) Lee, C.; Yang, W.; Parr, R. G. *Phys. Rev. B* **1988**, *37*, 78.

(21) BLYP calculations were performed with DGauss, a program that is part of the UniChem suite and is available from Accelerys: Andzelm, J.; Wimmer, E.; Salahub, D. R. In *The Challenge of d and f Electrons: Theory and Computations*; Salahub, D. R., Zerner, M. C., Eds.; ACS Symposium Series 394; American Chemical Society: Washington, DC, 1989; p 228. (b) Andzelm, J. In *Density Functional Methods in Chemistry*; Labanowski, J., Andzelm, J., Eds.; Springer-Verlag: New York, 1991. (c) Andzelm, J.; Wimmer, E. *J. Chem. Phys.* **1992**, *96*, 1280.

(22) Godbout, N.; Salahub, D. R.; Andzelm, J.; Wimmer, E. *Can. J. Chem.* **1992**, *70*, 560.

(23) (a) Peterson, K. A.; Woon, D. E.; Dunning, T. H., Jr. *J. Chem. Phys.* **1994**, *100*, 7410. (b) Woon, D. E.; Dunning, T. H., Jr. *J. Chem. Phys.* **1994**, *101*, 8877.

(24) Kim, K.; Friesner, R. A. *J. Am. Chem. Soc.* **1997**, *119*, 12952.

(25) Vargas, R.; Garza, J.; Friesner, R. A.; Stern, H.; Hay, B. P.; Dixon, D. A. *J. Phys. Chem. A* **2001**, *105*, 4963.

(26) Vargas, R.; Garza, J.; Dixon, D. A.; Hay, B. P. *J. Am. Chem. Soc.* **2000**, *122*, 4750.